Soft Matter

Cite this: *Soft Matter*, 2011, **7**, 3260

www.rsc.org/softmatter

REVIEW

Long-ranged electrostatics from local algorithms

Jörg Rottler*[a] and A. C. Maggs[b]

Received 24th September 2010, Accepted 1st December 2010
DOI: 10.1039/c0sm01057j

We show how to generate the long-ranged Coulomb interaction between pairs of particles with the help of an auxiliary field evolving with local dynamics. This allows one to simulate systems containing electric charges without ever calculating the Coulomb potential or solving Poisson's equation. The methods require the imposition of Gauss's law as a dynamical constraint on the auxiliary field. The local approach is particularly suited to treat implicit solvent models of dielectric media as well as Poisson–Boltzmann models of solutions. Generalizations to nonperiodic boundary conditions as well as practical aspects of the implementation are also reviewed.

1 Electrostatics from constrained energy functionals

Electrostatic interactions play a major role in controlling structure and properties of colloids, polyelectrolytes, membranes and many other soft materials. In computer simulations, the electrostatic potential energy is usually calculated *via* Coulomb's law, which is computed either through re-summation techniques[1] or equivalently by solving the Poisson equation.[2] Coulomb's law is often presented as a static limit of electrodynamics: charges moving with speed v create electromagnetic radiation; the charges are then stopped, allowing radiation to escape to infinity and then finally one measures the interaction energy $U_{ij} = q_iq_j/4\pi r_{ij}$ of the stationary charges.† Although the instantaneous Coulomb interaction is of course an excellent approximation in the context of condensed matter systems, a more general treatment, including retardation in the non-static case, generates corrections of order $(v/c)^2$, where c is the speed of light.[3] In fact these so-called Darwin interactions contain a subtle conceptual error: they assume motion in a radiationless background. When one looks at the interaction in a thermalized background the Darwin corrections to the interaction disappear in thermodynamic averages.[4] The thermodynamic interaction generated by the full coupled particle-electromagnetic system is just given by instantaneous Coulomb interactions, without dynamic corrections. This result can be traced back to very early work by Bohr and van Leeuwen, who showed that magnetic interactions between bodies are rigorously zero in classical (non-quantum) mechanics.[5]

This physical fact has been turned around in recent years in order to develop a series of local electrostatic algorithms based on dynamic electric fields. These algorithms have the advantage of never having to compute long-ranged Coulomb interactions explicitly. They work by recognizing that electrostatics is generated automatically if one imposes a local conservation law or constraints on a vector field discretized on a lattice. One must thus very explicitly construct a dynamical system that is not fully ergodic, so that certain configurations are never visited during the simulation. In philosophy this is very close to lattice Boltzmann algorithms for generating hydrodynamics from discrete lattice dynamics,[6] which work by imposing local momentum conservation in collisions. In local electrostatics one introduces a discretized electric field $\mathbf{E}(\mathbf{r})$. In standard electrostatic solvers one then requires that the electric field is derived from a potential so that $\mathbf{E} = -\operatorname{grad}\phi$. In the local algorithm this is no longer the case, one only requires the local dynamical constraint of Gauss' law, $\operatorname{div}\mathbf{E}(\mathbf{r}) = \rho(\mathbf{r})$ is maintained at all times. As usual the electrostatic energy is given by $\mathcal{U}[\mathbf{E}] = \frac{1}{2}\int \mathbf{E}(\mathbf{r})^2 \mathrm{d}^3\mathbf{r}$. If one now considers the charge density $\rho(\mathbf{r}) = \sum_i q_i\delta(\mathbf{r} - \mathbf{r}_i)$ generated by

[a]*Department of Physics and Astronomy, The University of British Columbia, 6224 Agricultural Road, Vancouver, BC, V6T 1Z1, Canada*
[b]*PCT, Gulliver CNRS-ESPCI 10 rue Vauquelin, 75005 Paris, France*
† Throughout the paper we use units such that $\varepsilon_0 = 1$.

Jörg Rottler

Jörg Rottler received his PhD in Physics from Johns Hopkins University in 2003. After postdoctoral work at ESPCI in Paris and at Princeton University until 2005, he joined the Department of Physics and Astronomy at the University of British Columbia, where is currently Associate Professor. His research interests include the nonequilibrium dynamics of amorphous solids and glasses, multiscale modeling of growth phenomena and structural phase transformations, and new computational algorithms for electrostatic effects in soft materials.

point charges q_i at temperature T, it is easy to show[7] that the constrained partition function factorizes

$$\mathcal{Z}(\{\mathbf{r}_i\}) = \int \mathcal{D}\mathbf{E} \prod_{\mathbf{r}} \delta(\mathrm{div}\mathbf{E}(\mathbf{r}) - \rho(\{\mathbf{r}_i\}))e^{-\mathcal{U}/k_BT}$$
$$= \mathcal{Z}_{Coulomb}(\{\mathbf{r}_i\}) \times \mathcal{Z}_{trans}, \quad (1)$$

We see that Gauss's law is imposed on all configurations of the field **E**. Here, $\mathcal{Z}_{trans}$ contains an integration over all transverse (non-potential) field degrees of freedom $\mathbf{E}_{trans} = \mathbf{E} + \mathrm{grad}\,\varphi$ and $\mathcal{Z}_{Coulomb}$ is the partition function of the same physical system, with interactions mediated by instantaneous Coulomb interactions. Thus, correct Coulombic Boltzmann weights are generated if one allows these extra field degrees of freedom to fluctuate subject to Gauss's law; it is not necessary to remove them entirely. One then samples the full partition function by integrating finally over the position of the charges in eqn (1).

The interesting point of the formulation in terms of eqn (1) is that the constrained partition function is very easy to sample using just local updates to the particle positions and the electric field **E**. This is very different to standard electrostatic solvers where motion of a single particle modifies the electrostatic potential, ϕ globally. Thus eqn (1) forms the basis of a family of linear scaling algorithms, which simultaneously sample particle and electric field configurations either through Monte Carlo (MC) or molecular dynamics (MD). The motion of particles implies a current **J**, and the electric field must change (but only locally) to preserve the Gauss constraint. In order to fully sample the transverse degrees of freedom in the partition function one can add a second set of MC moves which update the electric field on the plaquettes of the discretizing lattice.[8] Such MC sampling results in diffusive dynamics of the electric field (see below) and is frequently employed in other problems in condensed matter physics involving constraints, *e.g.* quantum spin models.[9,10] In the MD case, it is natural and convenient to introduce the magnetic field **B** and to evolve both **E** and **B** using full (propagative) Maxwellian dynamics.[11] Gauss's law is preserved if obeyed as an initial condition, and the transverse field degrees of freedom are sampled at the same temperature as the particles. Alternatively, the speed of light c may be used as a dynamical optimization parameter. The electric field can then be annealed to follow the solution of the Poisson equation adiabatially, similar to the electron density following the positions of nuclei in the Car–Parrinello method.[12]

We note that there is one very non-intuitive point in the use of auxiliary field variables. In the final, implemented code one has to simulate *more* degrees of freedom than in the original system. Naively one would expect this to complicate and slow down a simulation. In practice the locality of the resulting algorithm simplifies the calculation of the energy, while the extra field variables have autocorrelation times which are usually much shorter than other hydrodynamic variables such as the density. We discuss this point further in section 5.

The present review highlights several areas of interest for the application of the local electrostatic approach. Section 2 discusses the treatment of dielectric properties in implicit solvent simulations. Section 3 explains how thermal Keesom and Casimir forces emerge naturally from the present formalism. Poisson Boltzmann simulations are described in Section 5, and some details of the implementations constructed so far are reviewed in Section 6.

2 Inhomogeneous dielectric media and non-local electrostatics

Polyelectrolytes and biopolymers in solution are often characterized by strong dielectric contrast between themselves and the solvent: a low dielectric hydrocarbon chain with dielectric constant $\varepsilon \approx 2$–5 is immersed in water with $\varepsilon \approx 80$. In a simulation where water is represented as an implicit solvent, this contrast must be represented by a spatially varying dielectric function $\varepsilon(\mathbf{r})$, which also changes dynamically. The electrostatic energy of charges in such an inhomogeneous dielectric medium reads

$$\mathcal{U}[\mathbf{D}] = \int \frac{\mathbf{D}^2(\mathbf{r})}{2\varepsilon(\mathbf{r})} \mathrm{d}^3\mathbf{r} \quad (2)$$

where $\mathbf{D}(\mathbf{r}) = \varepsilon(\mathbf{r})\mathbf{E}(\mathbf{r})$ is the electric displacement that obeys the Gauss constraint, $\mathrm{div}\mathbf{D}(\mathbf{r}) = \rho(\mathbf{r})$. Since the Fourier transform no longer diagonalizes the corresponding Poisson equation $\mathrm{div}(\varepsilon(\mathbf{r})\mathrm{grad}\,\phi) = -\rho(\mathbf{r})$, many coarse-grained simulations ignore this contrast and use a uniform dielectric background instead. By contrast, the local electrostatic algorithm can easily treat any dynamical dielectric function by replacing **E** with **D** and using the electrostatic energy eqn (2) in eqn (1).[13–15]

An alternative, and more general approach to simulating dielectric effects consists of introducing a macroscopic polarization field[16,17] $\mathbf{P}(\mathbf{r})$ so that $\mathbf{D}(\mathbf{r}) = \mathbf{E}(\mathbf{r}) + \mathbf{P}(\mathbf{r})$. This allows one to couple a short-ranged Landau-Ginzburg approach to the local ordering of the dielectric together with a coupling of the induced charge $\rho_i = -\mathrm{div}\mathbf{P}$ to the long-ranged electrostatic fields. The total electrostatic energy thus reads

$$\mathcal{U}[\mathbf{D},\mathbf{P}] = \frac{1}{2}\int \mathrm{d}^3\mathbf{r}\,(\mathbf{D}(\mathbf{r}) - \mathbf{P}(\mathbf{r}))^2$$
$$+\frac{1}{2}\int \mathrm{d}^3\mathbf{r} \int \mathrm{d}^3\mathbf{r}'\,\mathbf{P}(\mathbf{r})K(\mathbf{r},\mathbf{r}')\mathbf{P}(\mathbf{r}'). \quad (3)$$

The first term in the energy is just the electric field energy $\mathbf{E}^2/2$ whereas the short ranged kernel $K(\mathbf{r}, \mathbf{r}')$ describes the local interactions between polarization vectors in the medium. **D** must still be considered as constrained by Gauss law. Similar functionals have also been introduced in quantum chemistry.[18] The simplest possible form for K is a *local* form, $K(\mathbf{r}, \mathbf{r}') = \kappa(\mathbf{r})I\delta(\mathbf{r}, \mathbf{r}')$ and eqn (3) is equivalent to eqn (2) with $\varepsilon(\mathbf{r}) = 1 + \kappa(\mathbf{r})^{-1}$. An advantage of eqn (3), however, is, that it provides a convenient starting point to treat *nonlocal* electrostatics,[19,20] where one must compute

$$\mathbf{D}(\mathbf{r}) = \int \mathrm{d}^3\mathbf{r}'\varepsilon(\mathbf{r},\mathbf{r}')\mathbf{E}(\mathbf{r}'). \quad (4)$$

Obtaining a first principled expression for the non-local kernel $K(\mathbf{r}, \mathbf{r}')$ is a difficult task, since it ultimately involves microscopic physics. If one assumes isotropy, however, one can in the spirit of Landau–Ginzburg theories with vector order parameters perform an expansion in derivatives of **P**. Such derivative couplings can have drastic effects on interactions at the nanometric scale. A classic, and very important, example is water: the

Fourier transform of the function $\varepsilon(\mathbf{r}-\mathbf{r}')$, $\varepsilon(\mathbf{q})$ displays a number of exceptional properties, including changes of sign and divergences as specific wave-vectors, before converging to unity for large wave-vectors.[21–23]

The main qualitative features of the dielectric response of bulk water can be reproduced with the present formalism.[24] Since the dielectric response involves the longitudinal degrees of freedom of the polarization we can further expand K in powers of div $\mathbf{P}$. The simplest functional that describes the above phenomenology of water is then

$$\frac{1}{2}\int d\mathbf{r}\int d\mathbf{r}'\mathbf{P}(\mathbf{r})K(|\mathbf{r}-\mathbf{r}'|)\mathbf{P}(\mathbf{r}') \approx \frac{1}{2}\int d\mathbf{r}[\kappa\mathbf{P}(\mathbf{r})^2+\kappa_l(\mathrm{div}\mathbf{P})^2+\alpha(\mathrm{grad}\ \mathrm{div}\mathbf{P})^2]. \quad (5)$$

Similar couplings in curl $\mathbf{P}$ can also be expected for the transverse field, but they do not modify the dielectric response in simple geometries. In most materials one would expect that $\kappa_l > 0$ and one can truncate the expansion after the first derivative contribution. The exceptional properties of water come from the fact that $\kappa_l < 0$. This requires the use of the third, higher derivative, contribution to the free energy in order to maintain thermodynamic stability. Such negative derivative couplings in Landau–Ginzburg expansions remind one of Lifshitz points in the theory of phase transitions where a susceptibility diverges at a finite wave-vector. Indeed in water it is known that such a giant susceptibility exists for $k \sim 0.7\ \mathrm{nm}^{-1}$. It is linked to fluctuations in the hydrogen bonding network which leads to a true critical point in the six vertex model.[25] The energy functional eqn (5) has been used to calculate the dielectric barrier for ion transport through an idealized low-dielectric membrane channel.[26] A difficulty with this approach is, however, that it cannot be expected to be accurate in the immediate vicinity of ions, where the structure of the solvent is strongly modified by steric effects and the presence of large electric fields.[27]

3 Fluctuations in dielectrics: thermal Keesom and Casimir potentials

We now turn to the finite temperature properties of functionals such as eqn (3). If we integrate over the field $\mathbf{D}$ in a partition function[24] we find that the local contribution to the free energy eqn (5) is supplemented with the electrostatic energy

$$U_c = \frac{1}{2}\int \frac{\mathrm{div}\mathbf{P}(\mathbf{r})\mathrm{div}\mathbf{P}(\mathbf{r}')}{4\pi|\mathbf{r}-\mathbf{r}'|}\,\mathrm{d}^3\mathbf{r}\mathrm{d}^3\mathbf{r}' = \frac{1}{2}\int \left|(\hat{\mathbf{q}}\cdot\mathbf{P}(\mathbf{q}))\right|^2\mathrm{d}^3\mathbf{q} = \frac{1}{2}\int \mathbf{P}(\mathbf{r})T(\mathbf{r}-\mathbf{r}')\mathbf{P}(\mathbf{r}')\,\mathrm{d}^3\mathbf{r}\mathrm{d}^3\mathbf{r}' \quad (6)$$

where T is the dipolar operator

$$T_{ij}(\mathbf{r}) = \frac{\delta_{ij}-3\hat{\mathbf{r}}_i\hat{\mathbf{r}}_j}{4\pi r^3}+\frac{\delta_{ij}}{3}\delta(\mathbf{r}). \quad (7)$$

If we combine the delta-function of eqn (7) with the local contribution in κ of eqn (5) one immediately finds the well known Clausius–Mossotti relation.

$$\frac{1}{\rho\alpha} = \frac{1}{3}+\kappa = \frac{1}{3}+\frac{1}{\chi} \quad (8)$$

relating the polarizability α to the susceptibility χ and the density of dipoles ρ.

It is known since the work of Keesom that a set of interacting, classical dipoles fluctuating at thermal equilibrium give rise to an effective potential of the form,[13]

$$V(r) = -\frac{\langle\mathbf{p}_i^2\rangle\langle\mathbf{p}_j^2\rangle}{3k_BT(4\pi r^3)^2} \quad (9)$$

where $\langle\mathbf{p}^2{}_i\rangle$ is the fluctuation of the dipole i in free space. We see that dielectric functionals based on the constrained electrostatic formalism must contain such potentials and are identical in content to standard models of fluctuating dipoles. In certain physical situations (such as solutions of lipid membranes) these interactions dominate the van der Waals interactions.[15]

If we integrate over the polarization field in a dielectric medium, eqn (3) reduces to eqn (2) which can also be shown to produce interactions decaying in $1/r^6$ in dielectric media.[13] This contradicts statements[14,28] that such dipolar terms are spurious artefacts of the constrained formalism. Such thermal interactions are often given the generic name of *Casimir* interactions. In general they give rise to non-pairwise potentials which are difficult to evaluate in general geometries. These interactions are automatically summed to all orders in the constrained algorithm. They can also be studied in detail using methods based on matrix factorization.[29] These thermal Casimir interactions should be distinguished from those generated by quantum fluctuations, the London dispersion interaction. In the context of simulations they require a full path integral treatment.[30]

In a uniform, isotropic dielectric medium fluctuations of the $\mathbf{P}$ field can be decomposed into longitudinal and transverse parts. The decomposition can be done in Fourier space defining the longitudinal component $\mathbf{P}_l = \hat{\mathbf{q}}(\hat{\mathbf{q}}\cdot\mathbf{P})$ and its complement the transverse component $\mathbf{P}_t = \mathbf{P} - \mathbf{P}_l$. Equivalently, one can use the dipolar operator T in a real-space projection: $\mathbf{P}_l = T\mathbf{P}$. The statistical mechanics of the transverse and longitudinal components is rather different. The energy for longitudinal fluctuations takes the form

$$U_l = \frac{1}{2}\sum_q \mathbf{P}_l(\mathbf{q})(1+K_l(\mathbf{q}))\mathbf{P}_l(-\mathbf{q}). \quad (10)$$

where the extra contribution proportional to unity comes from eqn (6). The subscript l on K_l reminds us that in the derivative terms in the energy only longitudinal contributions, such as div$\mathbf{P}$ couple to the fluctuations.

When the transverse degrees of freedom of the $\mathbf{D}$-field are integrated over, the effective energy is then

$$U_t = \frac{1}{2}\sum_q \mathbf{P}_t(\mathbf{q})K_t(\mathbf{q})\mathbf{P}_t(-\mathbf{q}). \quad (11)$$

We see that the unity term is not present, since the transverse fluctuations do not produce induced charges and do not contribute to the energy eqn (6). K_t includes contributions to the transverse energy such as those in curl $\mathbf{P}$. Thus we expect for $\mathbf{q} \neq 0$ K_l and K_t are different and that $K_t - K_l = O(q^2)$.

In conclusion, we deduce that the longitudinal and transverse fluctuations have a very different nature so that

$$\langle \mathbf{P}_l \cdot \mathbf{P}_l \rangle = \frac{kT}{1 + K_l(\mathbf{q})} \tag{12}$$

$$\langle \mathbf{P}_t \cdot \mathbf{P}_t \rangle = \frac{2kT}{K_t(\mathbf{q})}. \tag{13}$$

This implies the following fluctuation dissipation relation for the polarization fluctuations at long wavelengths (where K_l and K_t are identical),

$$\lim_{\mathbf{q}\to 0} \langle \mathbf{P}^2 \rangle = \frac{k_B T \varepsilon}{(2\varepsilon + 1)(\varepsilon - 1)}, \tag{14}$$

where we have used the fact that in the long wavelength limit the dielectric constant is $\varepsilon = 1 + K^{-1}$. The rational combination of ε is familiar from the theory of the Kirkwood g-function.[31]

4 Poisson–Boltzmann simulations

As well as replacing explicit solvent degrees of freedom by an effective dielectric medium, it is sometimes useful to coarse grain charge degrees of freedom in electrolytes. This is often done with the Poisson–Boltzmann equation. Standard formulations of the Poisson–Boltzmann method applied to electrolytes lead to challenging problems in applied mathematics: a non-linear partial differential equation must be solved for the potential at each time step of the simulation.[32] This typically involves the use of iterative solvers on large sets of discretized equations. A constrained variational formulation leads instead to simpler and more efficient formulations of the problem.

It is often convenient to construct a free energy for an electrolyte in a manner which is consistent with the Poisson–Boltzmann equation. Conventionally the Gibbs free energy of an electrolyte is expressed in terms of a functional of the electrostatic potential,[33–35]

$$G = \int \left\{ \rho_f \phi - \varepsilon \frac{(\mathrm{grad}\ \phi)^2}{2} - \sum_i kT \left\{ c_i^0 \left(e^{-q_i \phi / k_B T} - 1 \right) \right\} \right\} \mathrm{d}^3\mathbf{r} \tag{15}$$

where ρ_f is the external charge density and c_i^0 is the reference density of species i in the solution. By taking variations with respect to the potential ϕ one then finds the conventional Poisson–Boltzmann equations. This functional is numerically awkward,[36] in particular the stationary solution is not a minimum of the functional. This requires the use of sophisticated iterative solvers[37] in order remain thermodynamically consistent and excludes a Car–Parrinello approach, which could be potentially simpler and more efficient to implement.

The constrained formulation

$$G = \int \left\{ k_B T \sum_i c_i \ln\left(c_i / c_i^0\right) + \frac{\mathbf{D}^2}{2\varepsilon} \right\} \mathrm{d}^3\mathbf{r} \quad \text{with} \quad \mathrm{div}\mathbf{D} = \sum_i c_i q_i + \rho_f \tag{16}$$

leads instead to a true minimum principle for the energy. The authors of ref. 38 showed that a local minimization scheme easily converges to the correct solution of the Poisson–Boltzmann equation. Their formulation generalizes to a Car–Parrinello approach in which one can introduces fictitious kinetic terms in the energy.

Rather than interpreting the functional eqn (16) as a minimum it can also be interpreted as a coarse-grained energy[13] valid at finite temperatures. In this case one samples the charge degrees of freedom with Monte Carlo or molecular dynamics, and there is no need to solve the Poisson–Boltzmann equation at each time step, nor to perform a global minimization. One can anticipate considerable time savings in implicit solvent simulations.

5 Numerical implementation

Implementations of the local electrostatic algorithms begin with discretization of charges and fields on a cubic electric grid. Charges q_i reside on the nodes, while the electric field components E_{ij} may be associated with the links connecting the nodes i and j. At all times, the electric field must obey a discretized version of Gauss's law,

$$\sum_j E_{ij} = q_i / h^2, \tag{17}$$

where h is the grid spacing and the sum runs over nearest neighbor sites. The dynamical evolution of charges and fields depends on the simulation method of choice.

5.1 Monte Carlo for charged lattice gases

Monte Carlo sampling of eqn (1) can be performed with the following two elementary updates.[7] First, a charge q_i is moved from site i to site j and the electric field on the traversed link is updated according to $E_{ij} \to E_{ij} - q_i/h^2$ to maintain the Gauss constraint as depicted in Fig. 1. Additionally, an integration over the transverse field degrees of freedom must be performed. By grouping four fields into a plaquette and incrementing two of them by Δ while simultaneously decrementing the other by $-\Delta$, it is evident from Fig. 1 that Gauss's law remains satisfied at each vertex and only the rotational field components are changed. Both moves are manifestly local so that the energy change can be easily computed from the discretized energy $\mathcal{U} = \sum_i h^3 E_{ij}^2/2$. Moves are accepted or rejected according to the usual Metropolis rule.

5.1.1 Equilibration of transverse degrees of freedom. We have introduced a set of Monte Carlo updates that achieve the same result as Maxwell's equations: interactions are generated dynamically, they propagate but they generate an effective thermodynamic interaction equivalent to the conventional (static) Coulomb potential. One can ask what are the continuum evolution equations which correspond to this discrete dynamical system? Certainly a detailed understanding of the dynamics is needed to estimate the equilibration time of a simulation. As is often the case in MC algorithms, the dynamics are diffusive. The effective Langevin equation for the **E**-field can be shown to be[8,39]

$$\frac{\partial \mathbf{E}}{\partial t} = \left(\nabla^2 \mathbf{E} - \nabla\rho\right)/\xi - \mathbf{J} + \ \mathrm{curl}\ \eta/\xi, \tag{18}$$

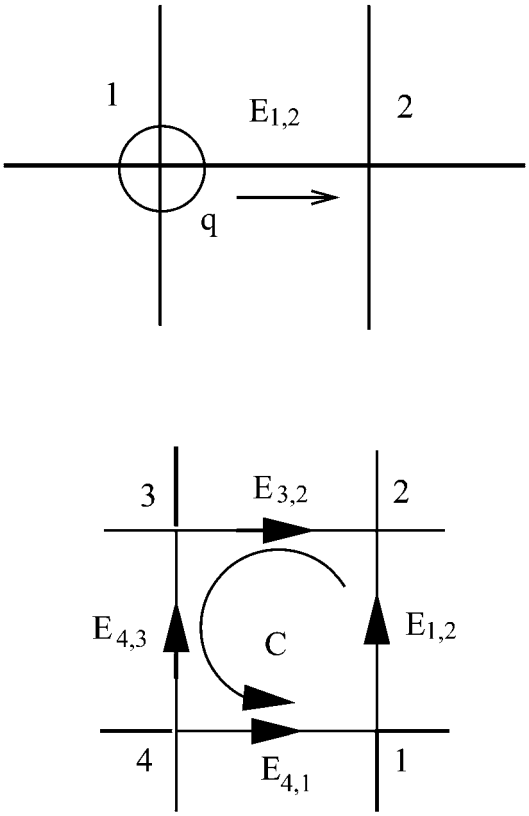

Fig. 1 Constrained charge and field updates in MC simulations. Moving a charge from site 1 to 2 requires modification of the electric field on the traversed link. Changing the electric field on the links $E_{1,2}$ and $E_{4,1}$ by Δ and on $E_{3,2}$ and $E_{4,3}$ by $-\Delta$ only changes the rotational (curl) degrees of freedom. Reproduced from ref. 7, © 2002 by the American Physical Society.

where ξ is a relaxation time that can be controlled by the frequency of transverse field updates and η is a a vector of white noise. One notes that in the absence of current and noise the static solution is consistent with the Poisson equation for the electric field, and on taking the divergence of the equation one sees that it is indeed compatible with the constraint of Gauss's law.

Solutions to this equation are particularly interesting in the presence of free ions in an electrolyte, characterized by a finite conductivity σ. In this case $\mathbf{J} = \sigma\mathbf{E}$. Upon Fourier transforming, one finds the relaxation time $\tau_q = \xi/(q^2 + \sigma)$ for modes of wave-vector q. From the original diffusion equation one could have guessed that the electric field has a equilibration time which diverges with the system size L as L^2. The criterion for equilibration is in fact much easier to obtain: the free ions must diffuse further than the Debye length. Long wavelength modes decay at a rate which is independent of the system size due to the appearance of a gap in the spectrum. We interpret this gap as the diffusive equivalent of the plasmon mode found with Maxwell's equations. Careful tests of the algorithm[39] showed that for reasonable ratios of particle to field updates, convergence is actually limited by the particle degrees of freedom, whose relaxation times also increase quadratically with system size.

Further improvements to transverse field equilibration in the absence of free ions can be achieved by introducing global constrained field updates similar in spirit to worm algorithms.[9,40] The plaquette update shown in Fig. 1(b) is only the simplest kind of update that preserves Gauss's law. These local moves may be supplemented with a cluster update that nucleates a pair of positive and negative pseudo-particles on the lattice. One of the particles then performs a random walk biased by the energy, and the field on each traversed link is updated as before. When the particle meets the stationary partner again, Gauss's law is satisfied and the entire update is either globally accepted or refused. These updates equilibrate the transverse field equally fast on all length scales with minimal overhead.[41] An alternative approach suggests global updates of the transverse field of freedom *via* Fast Fourier Transforms.[42]

5.1.2 Improving charge mobility. The algorithm as described so far is not yet suitable for the simulation of Coulomb gases at coupling strengths typical for many lattice models of charged media:[44] the algorithm has a kinetic barrier. Motion of a particle between two sites of the lattice leads to a finite energy difference which implies that the acceptance rate falls off exponentially at low temperatures. Additionally, consecutive motion of charges leaves behind a field trail whose energy cost grows linearly with the number of steps. If the trail is not dispersed quickly by transverse field updates or by other charges moving in the vicinity, the charge mobility is greatly reduced. Both these problems can be solved by introducing temporary charge spreading.[43] In this method, illustrated in Fig. 2, a charge is first spread evenly onto w^3 neighboring sites. The charge cloud is then moved as a block and recondensed at the final position. Gauss's law must be maintained during each step. While the field on each link during step 2 changes simply by q/h^2w^3, the currents $j_i^{(1,3)}$ during expansion (1) and contraction (3) are under-determined. One possible choice for j_i comes from minimizing $\sum_i (j_i^{(1,3)})^2/2$; the associated Poisson problem can be solved at the beginning of the simulation.[43] The above procedure reduces the dynamic barrier by a factor w^2, and a value of $w = 5$ is recommended for optimal efficiency. A closely related coupled particle-field update procedure was also suggested in ref. 45.

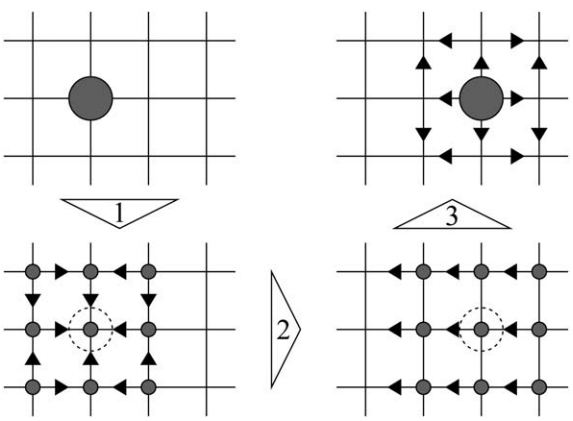

Fig. 2 Scheme for temporary charge spreading (see text). Reproduced from ref. 43, © 2005 by the American Physical Society.

5.2 Molecular dynamics

For molecular dynamics, we sample eqn (1) by directly integrating Maxwell's equations coupled to the equations of motion for the charges q_i of mass m_i,

$$\dot{\mathbf{B}} = -c \ \ \text{curl} \ \mathbf{E} - \gamma_2 \mathbf{B} + \vec{\xi}_2, \quad m_i \dot{\mathbf{v}}_i = q_i \mathbf{E}(\mathbf{r}_i) - \gamma_1 \mathbf{v}_i + \vec{\xi}_1,$$
$$\dot{\mathbf{E}} = c \ \ \text{curl} \ \mathbf{B} - \mathbf{J}, \qquad \dot{\mathbf{r}}_i = \mathbf{v}_i. \tag{19}$$

The electric field **E** obeys Gauss's law as an initial condition, which is conserved by the above dynamics. Although the Lorentz force has been dropped in the electrostatic limit, it can be shown that the above equations of motion obey a generalized Liouville dynamics.[11] Both the charges and the magnetic field **B** have additionally been coupled to Langevin thermostats, where the dampings γ_i and noise terms ξ_i are related by the fluctuation dissipation theorem. Coupling the magnetic field to a thermostat opens the way to running the algorithm in two modes. Maintaining the field degrees of freedom at the same temperature ensures ergodicity and the correct equilibrium ensemble is guaranteed independent of the value chosen for the speed of light c. Alternatively, the electric field can be annealed to zero temperature by setting the noise term ξ_2 to zero; in this case the field always remains close to the solution of Poisson's equation.[11]

Maxwell's equations are integrated using the well-known algorithm due to Yee,[46] where the electric and magnetic fields are associated with the links and faces of a cubic grid, respectively.[11,47] A velocity Verlet method can then be used to advance the fields. An alternative implementation by Pasichnyk and Dünweg uses an equivalent vector potential formulation.[48] Stable integration requires the time-step δt to obey the Courant condition, $\delta t < h/\sqrt{3}c$. Thus reasonable time-steps require choosing values of c much smaller than the speed of light; in practice of order the particle velocity. The precise optimization depends on the extent to which dynamical correlations are to be resolved. The full algorithm combines the field integration with a velocity Verlet step for the particles, see ref. 47 for details.

5.3 Charge and current interpolation, accuracy, and efficiency

In MD simulations as well as in off-lattice MC simulations, particles move in the continuum. Interpolation of charges and currents to the electric grid and extrapolation of energies and forces represent the major technical challenge for the algorithms. Point charges must be interpolated as a charge cloud over a support of finite width, and a local current **J** must flow so that the constraint div**J** = $-\Delta\rho$ is obeyed at each site and time-step. Early implementations used a low-order B-spline interpolation combined with a regularization of the Coulomb potential at short distances *via* a scalar field to minimize lattice artefacts and aliasing errors.[11,39] At this level of interpolation, all major features of Coulombic systems are reproduced. Fig. 3 illustrates for instance Debye screening in a symmetric electrolyte at different concentrations and shows in the inset a direct comparison between the electrostatic force between a pair of ions generated by the algorithm and an analytic Ewald summation. To improve accuracy, more recent incarnations used instead Gaussian charge spreading over the lattice.[47,49] Gaussian charge clouds relate directly to the Ewald-formula, and their aliasing

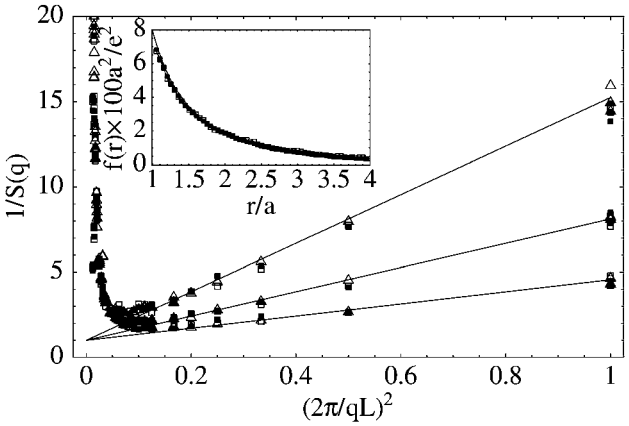

Fig. 3 Static structure factor of a symmetric electrolyte at three different densities obtained from MD simulations using the local algorithm. □: particle and fields thermostatted to the same temperature, ■: electric field is damped (see text), Δ: results from corresponding MC simulation. Solid lines show predictions of the Debye theory. The inset shows the average instantaneous force in both modes. The solid curve shows the force resulting from the potential $V = -1/4\pi r - r^2/6L^3$ from Ewald summation. Reproduced from ref. 11, © 2004 by the American Physical Society.

error decreases more rapidly with the Gaussian width than for n-splines. When combined with a higher order approximation for the discretized Laplacian operator, absolute rms errors of the forces and energies of order $O(10^{-2}-10^{-4})$ can be realized.[47,49] Achieving high accuracy requires interpolation over a very large support, since real space solvers lack efficient error subtraction methods that are available to Fourier-based methods.

The local algorithms exhibit true linear scaling in both MC and MD versions. The prefactor depends on the desired level of accuracy. The locality also makes parallelization over many processors extremely easy. A parallelized implementation was found to compete well against a conventional PPPM electrostatic solver at rms force errors of $O(10^{-3})$.[47] Without further improvements of the charge interpolation scheme, however, present implementations do not offer significant speed advantages in standard 3D-periodic electrostatic situations for *in vacuo* simulations.

5.4 Non-periodic boundary conditions

A final appealing advantage of the local electrostatic approach consists in its flexibility in the implementation of heterogeneous boundary conditions. Coulomb solvers relying on the Fast Fourier Transform have difficulty dealing with exotic boundary conditions: geometries without separable coordinate systems, electrodes, and highly anisotropic geometries such as two dimensional slabs. In particular the local MC algorithm can quite easily accommodate quasi-two dimensional systems embedded in three dimensional space by extending the electric grid in one periodic direction and restricting particle positions to the thin slab.[50] By padding the system with empty space, interactions between the periodic images fall off exponentially, and in practice a threefold increase of the simulation box in the direction normal to the slab is sufficient. Field equilibration in the

empty space can be efficiently performed with the worm algorithm, and the results are formally equivalent to use of the Ewald sum.[51]

Metallic boundary conditions at either constant charge or constant potential have also been studied. Such boundary conditions represent systems confined between electrodes. For a surface charge density $\sigma(\mathbf{r})$, the electric field must obey Dirichlet boundary conditions,

$$\mathbf{E}(\mathbf{r})\cdot\hat{\mathbf{n}}(\mathbf{r}) = -\sigma(\mathbf{r}), \tag{20}$$

where $\hat{\mathbf{n}}$ is an outward facing unit surface normal. In the simulation, the electric grid is terminated at the surfaces, and mobile surface charges confined to the plane are added to render the surface metallic.[45,51] Constant potential boundary conditions at an externally imposed potential $\phi_{(ext)}$ can be obtained through a Legendre-transform that lets the surface charge density fluctuate,[50]

$$U[\mathbf{E},\sigma] = U[\mathbf{E}] - \oint_S \sigma\phi_{(ext)}\mathrm{dS}. \tag{21}$$

This requires introducing a global MC move that transfers charge from one surface to another, just like the current generated by a battery. Accordingly, the electric field changes everywhere in the simulation cell, but the update does not dominate the total simulation time. Using this method, simulations of the electric double layer at various coupling strengths were successfully performed, including in the regime of attractive interactions between like-charged walls.[51]

6 Perspectives

Coulomb's law without dynamic (Darwin) corrections arises naturally from electrodynamics in a thermalized background. By reintroducing either diffusive or propagative field dynamics, electrostatic interactions can be generated with local algorithms that guarantee the correct equilibrium ensemble independent of the propagation speed of the fields. The algorithms exhibit true linear scaling with the number of charges, with the prefactor determined by the desired accuracy. With dynamical charge spreading, efficient Monte Carlo simulations of charged lattice gases at temperatures typical for soft condensed matter systems are possible. The algorithm generates Coulombic interactions in any dimensions; recent applications include a study of vortex dynamics and the Nernst effect in two-dimensional superconductors.[52]

In the context of off-lattice simulations, the biggest potential of the local electrostatic methods described here lies in their greater flexibility with treating non-periodic boundary conditions and their ability to treat dielectric effects in implicit solvent simulations that retain all ionic species, but treat the solvating water molecules only on the continuum level. Here the algorithm competes with other real-space approaches such as multigrid methods.[53] Since fully atomistic simulations are fundamentally limited in length and time scales, systematically coarse-grained models that preserve important nanoscale physics can be expected to assume a greater role in the future. Importantly, nonlocal effects, which are ignored in virtually all implicit models to date, can be systematically included. In cases where counterions do not need to be represented explicitly, the approach also opens the door to more efficient simulations on the Poisson–Boltzmann level.

References

1 J. W. Perram, H. G. Petersen and S. W. de Leeuw, *Mol. Phys.*, 1988, **65**, 875–889.
2 U. Essmann, L. Perera, M. L. Berkowitz, T. Darden, H. Lee and L. G. Pedersen, *J. Chem. Phys.*, 1995, **103**, 8577–8593.
3 J. D. Jackson, *Classical Electrodynamics*, Wiley, 1999.
4 A. Alastuey and W. Appel, *Phys. A*, 2000, **276**, 508–520.
5 J. H. V. Vleck, *The Theory of Electric and Magnetic Susceptibilities*, Oxford University Press, Oxford, 1932.
6 U. Frisch, B. Hasslacher and Y. Pomeau, *Phys. Rev. Lett.*, 1986, **56**, 1505–1508.
7 A. C. Maggs and V. Rossetto, *Phys. Rev. Lett.*, 2002, **88**, 196402.
8 A. C. Maggs, *J. Chem. Phys.*, 2002, **117**, 1975–1981.
9 F. Alet and E. S. Sørensen, *Phys. Rev. E: Stat. Phys., Plasmas, Fluids, Relat. Interdiscip. Top.*, 2003, **67**, 015701.
10 G. Chen, J. Gukelberger, S. Trebst, F. Alet and L. Balents, *Phys. Rev. B: Condens. Matter Mater. Phys.*, 2009, **80**, 045112.
11 J. Rottler and A. C. Maggs, *Phys. Rev. Lett.*, 2004, **93**, 170201.
12 R. Car and M. Parrinello, *Phys. Rev. Lett.*, 1985, **55**, 2471.
13 A. C. Maggs, *J. Chem. Phys.*, 2004, **120**, 3108–3118.
14 A. Duncan, R. D. Sedgewick and R. D. Coalson, *Phys. Rev. E: Stat., Nonlinear, Soft Matter Phys.*, 2006, **73**, 016705.
15 I. Pasichnyk, A. C. Maggs and R. Everaers, *J. Phys. Chem. B*, 2008, **112**, 1761.
16 M. Marchi, D. Borgis, N. Levy and P. Ballone, *J. Chem. Phys.*, 2001, **114**, 4377–4385.
17 P. Attard, *J. Chem. Phys.*, 2003, **119**, 1365–1372.
18 M. Stengel, N. A. Spaldin and D. Vanderbilt, *Nat. Phys.*, 2009, **5**, 304–308.
19 A. A. Kornyshev, *in: The Chemical Physics of Solvation. Part A: Theory of Solvation* (ed.: R. R. Dogonadze, R. Kalman, A. A. Kornyshev, and J. Ulstrup), Elsevier, Amsterdam, 1985, p. 77.
20 A. Hildebrandt, R. Blossey, S. Rjasanow, O. Kohlbacher and H.-P. Lenhof, *Phys. Rev. Lett.*, 2004, **93**, 108104.
21 P. A. Bopp, A. A. Kornyshev and G. Sutmann, *Phys. Rev. Lett.*, 1996, **76**, 1280.
22 O. V. Dolgov, D. A. Kirzhnits and E. G. Maksimov, *Rev. Mod. Phys.*, 1981, **53**, 81–94.
23 A. A. Kornyshev and G. Sutmann, *J. Chem. Phys.*, 1996, **104**, 1524.
24 A. C. Maggs and R. Everaers, *Phys. Rev. Lett.*, 2006, **96**, 230603.
25 R. J. Baxter, *Exactly Solved Models in Statistical Mechanics*, Dover Publications, 2007.
26 J. Rottler and B. Krayenhoff, *J. Phys.: Condens. Matter*, 2009, **21**, 255901.
27 M. V. Fedorov and A. A. Kornyshev, *Mol. Phys.*, 2007, **105**, 1.
28 A. Duncan and R. D. Sedgewick, *Phys. Rev. E: Stat., Nonlinear, Soft Matter Phys.*, 2006, **73**, 066711.
29 S. Pasquali and A. C. Maggs, *J. Chem. Phys.*, 2008, **129**, 014703.
30 H. Berthoumieux and A. C. Maggs, *Europhys. Lett.*, 2010, **91**, 56006.
31 J. G. Kirkwood, *J. Chem. Phys.*, 1939, **7**, 911–919.
32 K. A. Sharp and B. Honig, *J. Phys. Chem.*, 1990, **94**, 7684–7692.
33 M. K. Gilson, M. E. Davis, B. A. Luty and J. A. McCammon, *J. Phys. Chem.*, 1993, **97**, 3591–3600.
34 W. Im, D. Beglov and B. Roux, *Comput. Phys. Commun.*, 1998, **111**, 59–75.
35 E. S. Reiner and C. J. Radke, *J. Chem. Soc., Faraday Trans.*, 1990, **86**, 3901–3912.
36 F. Fogolari and J. M. Briggs, *Chem. Phys. Lett.*, 1997, **281**, 135–139.
37 R. Luo, L. David and M. K. Gilson, *J. Comput. Chem.*, 2002, **23**, 1244–1253.
38 M. Baptista, R. Schmitz and B. Dünweg, *Phys. Rev. E: Stat., Nonlinear, Soft Matter Phys.*, 2009, **80**, 016705.
39 J. Rottler and A. C. Maggs, *J. Chem. Phys.*, 2004, **120**, 3119–3129.
40 N. Prokof'ev and B. Svistunov, *Phys. Rev. Lett.*, 2001, **87**, 160601.
41 L. Levrel, F. Alet, J. Rottler and A. Maggs, *Pramana*, 2005, **64**, 1001–1010.
42 A. Duncan, R. D. Sedgewick and R. D. Coalson, *Comput. Phys. Commun.*, 2006, **175**, 73.
43 L. Levrel and A. C. Maggs, *Phys. Rev. E: Stat., Nonlinear, Soft Matter Phys.*, 2005, **72**, 016715.

44 E. Luijten, M. E. Fisher and A. Z. Panagiotopoulos, *Phys. Rev. Lett.*, 2002, **88**, 185701.
45 A. Duncan, R. D. Sedgewick and R. D. Coalson, *Phys. Rev. E: Stat., Nonlinear, Soft Matter Phys.*, 2005, **71**, 046702.
46 K. S. Yee, *IEEE Trans. Antennas Propag.*, 1966, **14**, 302–307.
47 J. Rottler, *J. Chem. Phys.*, 2007, **127**, 134104.
48 I. Pasichnyk and B. Dünweg, *J. Phys.: Condens. Matter*, 2004, **16**, S3999.
49 A. C. Maggs, *Phys. Rev. E: Stat., Nonlinear, Soft Matter Phys.*, 2005, **72**, 040201.
50 L. Levrel and A. C. Maggs, *J. Chem. Phys.*, 2008, **128**, 214103.
51 D. Thompson and J. Rottler, *J. Chem. Phys.*, 2008, **128**, 214102.
52 S. Raghu, D. Podolsky, A. Vishwanath and D. A. Huse, *Phys. Rev. B: Condens. Matter Mater. Phys.*, 2008, **78**, 184520.
53 C. Sagui and T. Darden, *J. Chem. Phys.*, 2001, **114**, 6578–6591.